Behavior Of Lens Aberrations As A Function Of Wavelength On KrF and ArF Lithography Scanners

Mark Terry, Ivan Lalovic*, Greg Wells, and Adlai Smith**
Texas Instruments, Inc., Dallas, Texas
*Cymer Inc., San Diego, California
**Litel Instruments Inc., San Diego, California

ABSTRACT

In this paper we study the effects of changing the operating laser wavelength on the projection lens aberrations of KrF and ArF scanners as measured by the Litel In-Situ Interferometer. Specifically, we quantify the change in 28 individual Zernike coefficients[1] as a function of wavelength as well as the total RMS. Effects on Zernike's exhibiting a field dependent behavior are described in detail. We convert the Z4 terms to Z positions to estimate the displacement of the image plane, and we identify a new chromatic distortion term. Finally, we input the measured wavefronts into a lithographic simulator to estimate the full effects on image placement error.

1. INTRODUCTION

As optical lithography projectors are increasingly required to print feature sizes below the illumination wavelength, the properties of the illumination spectrum can be expected to play a more significant role in the imaging performance. It is important then that the peak wavelength of an exposure tool be selected for the best possible imaging performance. In addition, as new materials are inserted into lens designs to accommodate smaller wavelengths, material properties will affect the wavelength sensitivity of designs to aberrations,[2] leading to more stringent requirements on the illumination spectrum. It is useful then to quantify the effects of changing the peak wavelength on the aberrations of current optical projectors.

In this work, we characterize and compare the aberrations of the lenses of a 248nm scanner, and a 1st generation 193nm scanner using the Litel ISI technique by measuring the wavefront as a function of wavelength. The Zernike coefficient values presented in this paper are not absolute, but are rather difference values computed as a difference from the Zernike coefficients measured at the nominal wavelength.

2. EXPERIMENTAL CONDITIONS

Data was collected from a 248nm and 193nm scanners using the Litel ISI technique for measuring wavefront aberrations on lithographic exposure tools. Table 1. summarizes the experiments.

Parameter	248nm	193nm
Wavelength Change	+/- 9pm	+/- 5pm
NA	.68	.60
Exposure	Static	Static

Table 1. Experiments performed with Litel ISI.

Figure 1 shows the across slit possible sampling locations of the ISI interferometer, along with the coordinate direction definitions, from which data for this paper was collected.

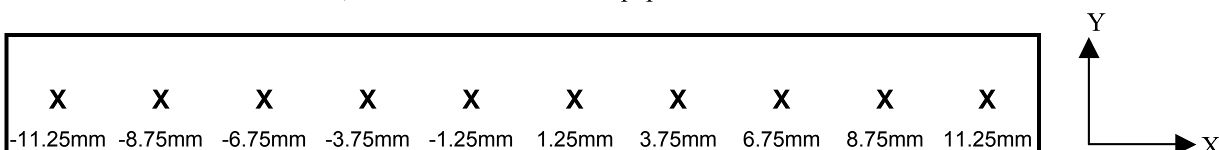

Figure 1. Typical across slit sampling pattern.

Optical Microlithography XIV, Christopher J. Progler, Editor, Proceedings of SPIE Vol. 4346 (2001)
© 2001 SPIE · 0277-786X/01/$15.00

3. EXPERIMENTAL RESULTS

3.1 Change In Zernike Coefficients

The Zernike coefficients for the sampled field points were averaged and plotted through wavelength. A linear fit was made to the average values and a slope, which corresponds to the rate of change of the coefficent per unit wavelength, was calculated. We are interested in looking at both average and across field effects, so we consider:

1. The average change in the Zernike coefficients considering all field points, and
2. Across field patterns in the Zernike coefficient data as a function of wavelength.

The average change in the coefficients for both 193nm and 248nm systems are shown in Table 2. The coefficients showing the most significant change are highlighted in black.

Zernike Coefficient	193nm mwaves/pm	248nm mwaves/pm	193/248 ratio
Z2	**0.7**	**-0.8**	2.7 (peaks)
Z3	**0.8**	**1.3**	1.1 (peaks)
Z4	**-86.9**	**-77.6**	1.1
Z5	0.1	0.1	1.5
Z6	**-0.5**	**-0.3**	1.4
Z7	**-0.3**	**0.2**	1.8
Z8	0.1	0.1	3.0 (peaks)
Z9	-0.1	0.0	
Z10	0.1	-0.1	
Z11	**-3.1**	**-3.2**	1.0
Z12	0.0	0.0	
Z13	0.0	0.1	
Z14	**0.2**	0.1	
Z15	0.1	0.0	
Z16	0.0	0.0	
Z17	0.0	0.0	
Z18	0.0	0.0	
Z19	0.0	0.0	
Z20	0.1	0.0	
Z21	0.1	0.0	
Z22	**-0.3**	**-0.2**	1.3
Z23	0.0	0.0	
Z24	0.0	0.0	
Z25	0.0	0.0	
Z26	0.0	0.0	
Z27	0.0	0.0	
Z28	-0.1	0.0	

Table 2. Average Change In Zernike Coefficient With Change In Wavelength (mwaves/pm)

The data in Table 2 shows that the lower order radially symmetric coefficients, Z4 and Z11, have the largest average change with wavelength. In general, the significant effects on the Zernike coefficients are limited to the lower orders. In addition, the 193nm Zernike coefficients were more sensitive to a change in wavelength as shown by the >1 values in the 193/248 ratio column. “Peaks” indicates that the peak values were used to calculate the ratio.

Across field effects were identified by visual inspection of the plotted data. Zernike terms Z2, and Z8 were determined to have a strong across field dependence for both 248nm and 193nm systems. Z3 also had an across field dependence for the 193nm system. These effects will be shown in more detail in the next section.

3.2 0 – θ Terms
Z4, Z11, Z22: Defocus, Primary Spherical, Secondary Spherical

As the wavelength of the illumination is varied, the image plane of the lens system changes as a result of the material dispersion of the lens elements. The movement of the image plane is reflected in the change in the Zernike coefficients for the radially symmetric terms Z4, Z11, and Z22. Figures 2 and 3 show the experimentally measured change in Z4, Z11, and Z22 sampled across the slit for 193nm and 248nm scanner lenses respectively.

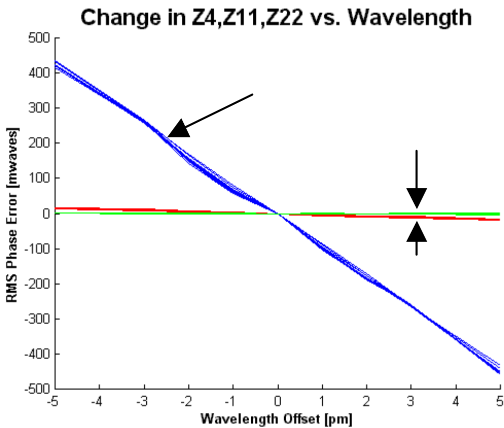

Figure 2. Change in Z4, Z11, and Z22 with wavelength on a 193nm scanner.

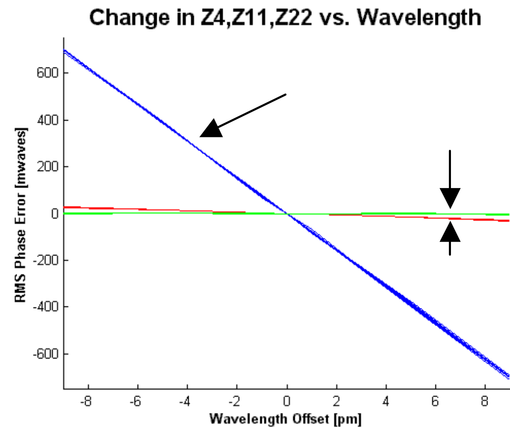

Figure 3. Change in Z4, Z11, and Z22 with wavelength on a 248nm scanner.

The figures illustrate that the change in Z4 is the dominant effect, and that the relative amount of change in Z4, Z11, and Z22 for both the 193nm and 248nm lenses is roughly the same. Figures 4 and 5 show the change in Z11 and Z22 for the 193nm lens plotted on smaller scales in order to illustrate the trend and the noise level for each of the data sets.

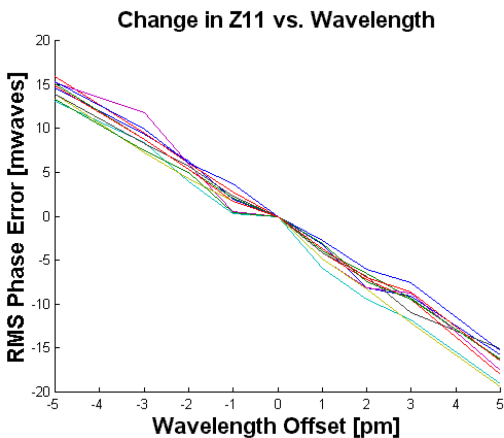

Figure 4. Change in Z11 with wavelength on a 193nm scanner.

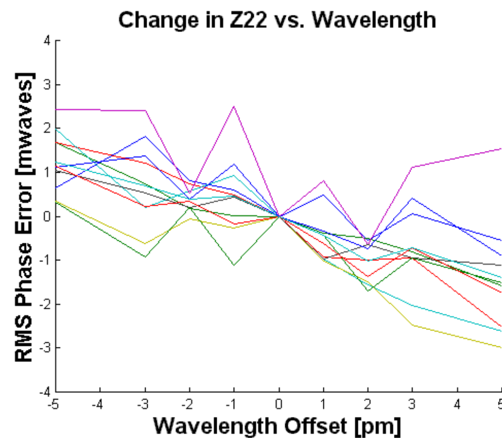

Figure 5. Change in Z22 with wavelength on a 193nm scanner

The coefficients for the radially symmetric terms did not show across field dependence with wavelength at 248nm or 193nm. Figures 6 and 7 show the change in Z4 and Z11 across the slit of a 193nm scanner. The change across the slit is similarly uniform for Z22 although the data is noisier.

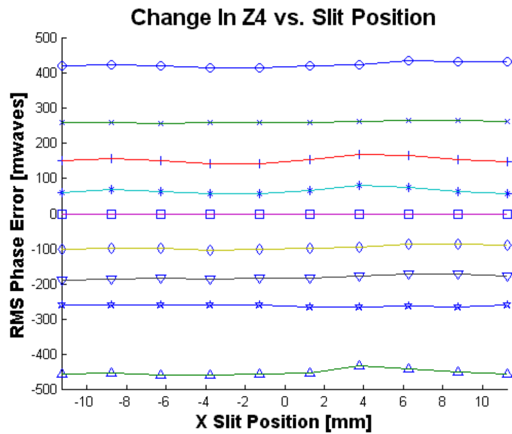

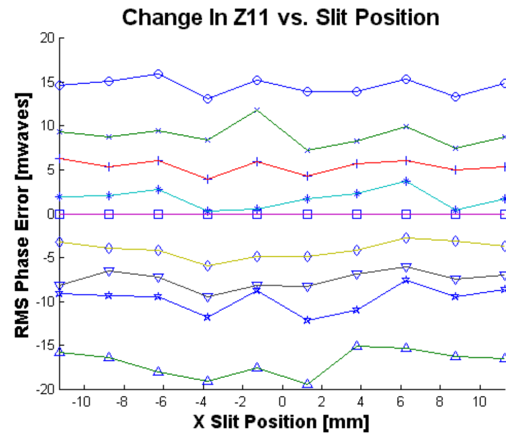

Figure 6. Across slit change in Z4 with wavelength on a 193nm scanner.

Figure 7. Across slit change in Z11 with wavelength on a 193nm scanner

Figure 8 shows a plot of the change in Z4 as a function of wavelength on the same set of axis for both the 193nm and 248nm systems.

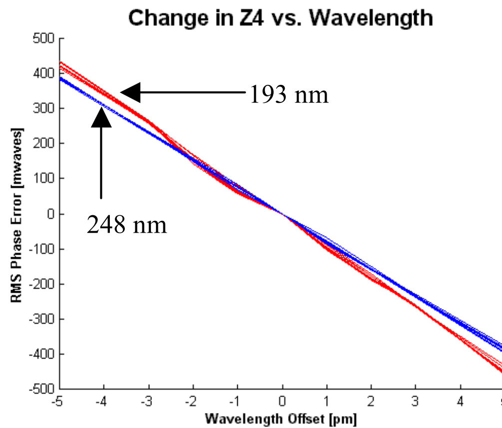

Figure 8. Change in Z4 with wavelength for 193nm and 248nm scanners.

3.3 1 – θ Terms

3.3.1 Z2 and Z8: X Tilt and X Coma

The changes in Z2 and Z8 as a function of slit position and wavelength for the 193nm scanner lens are shown in Figures 9 and 10 respectively. Both figures show a change with wavelength that is a strong function of slit position. The response is seen to be cubic or sinusoidal in shape. As one side of the slit changes in the positive direction, the other side of the slit changes in the negative direction. The peak change occurs near or at the edge of the slit

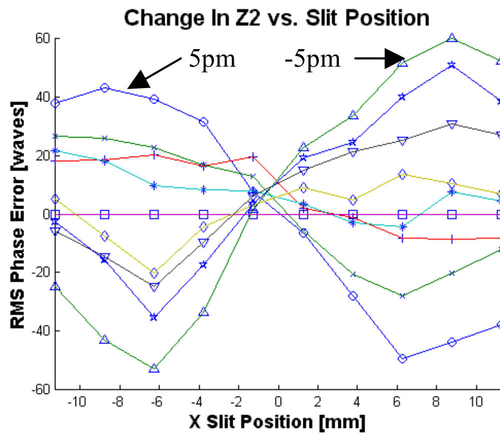

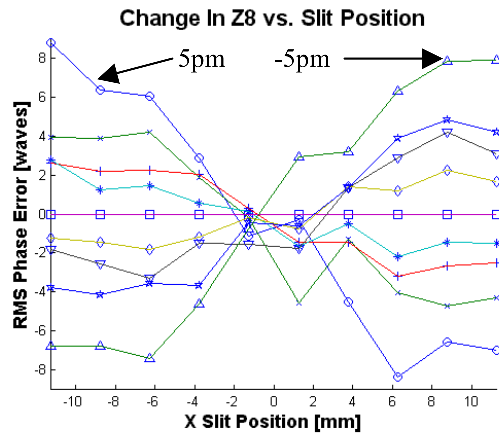

Figure 9. Across slit change in Z2 with wavelength on a 193nm scanner.

Figure 10. Across slit change in Z8 with wavelength on a 248nm scanner.

Figures 11 and 12 show the rate of change for the 248nm and 193nm lenses of Z2 and Z8 respectively. The max and min values for each are listed in Table 4.

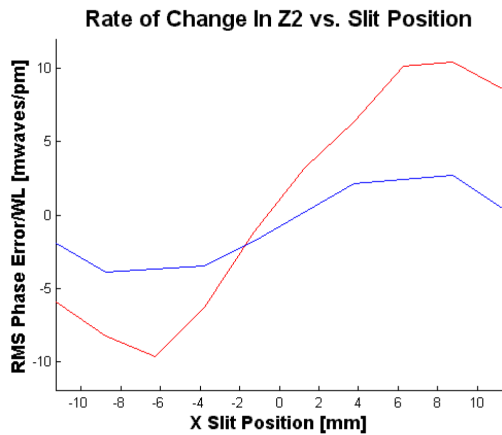

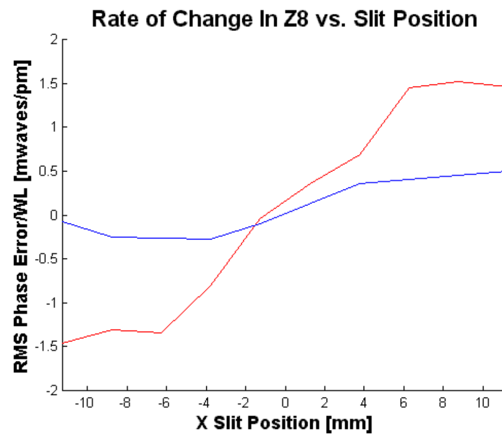

Figure 11. Rate of change of Z2 as a function of slit position for the 193nm and . 248nm lenses.

Figure 12. Rate of change of Z8 as a function of slit position for the 193nm and 248nm lenses.

	193nm [mwaves/pm]	248nm [mwaves/pm]
Z2 min	-9.7	-3.9
Z2 max	10.4	2.7
Z8 min	-1.5	-.3
Z8 max	1.5	.5

Table 4. Peak rates of change for Z2 and Z8 for 193nm and 248nm lenses.

3.3.2 Z3 and Z7: Y Tilt and Y Coma

Figures 13 and 14 show the rates of change for Z3 and Z7 respectively. A small field dependent trend for Z3 was detected for the 193nm system. Z3 dropped from a maximum rate of 1.9 mwaves/pm on the left side of the slit to .3 mwaves/pm on the right side of the slit.

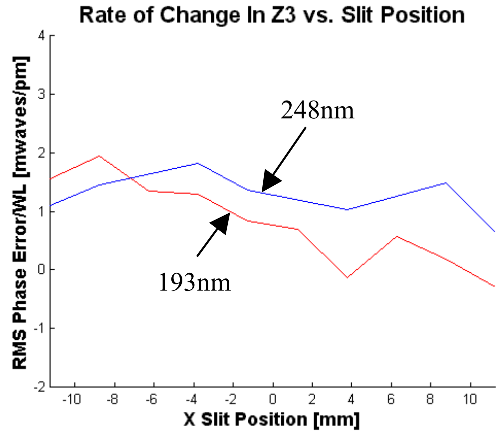

Figure 13. Rate of change of Z3 as a function of slit position for the 193nm and 248nm lenses.

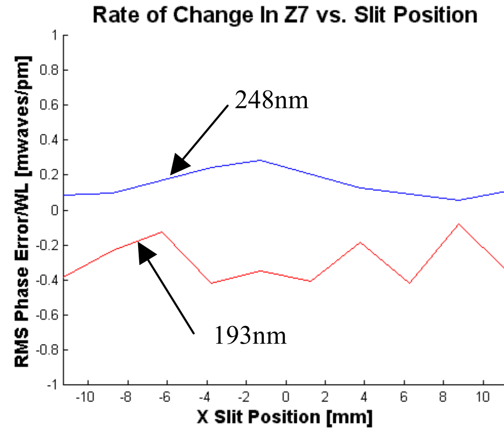

Figure 14. Rate of change of Z7 as a function of slit position for the 193nm and 248nm lenses.

3.4 Multi – θ Terms

3.4.1 Z6 and Z14: Astigmatism and X Quadrafoil

Figures 15 and 16 show the behavior of Z6 as a function of wavelength along with the noise level of the measurement. Figure 17 shows the behavior of X quadrafoil.

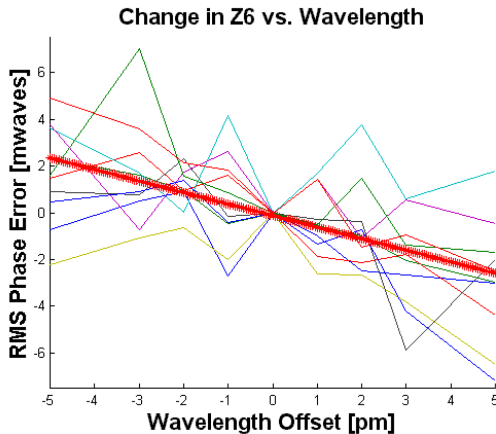

Figure 15. Change in Z6 with wavelength on a 193nm scanner.

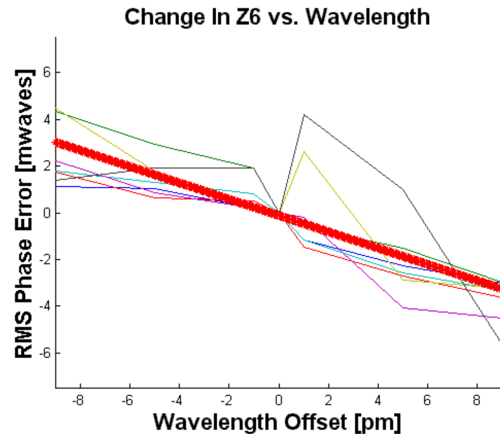

Figure 16. Change in Z6 with wavelength on a 248nm scanner.

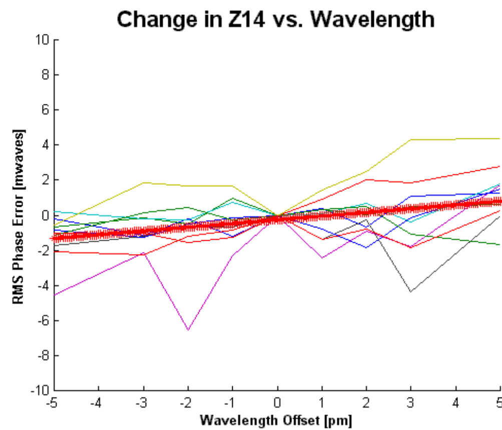

Figure 17 Change in Z14 as a function of wavelength for the 193nm lens.

3.5 Total RMS

The wavefronts at each field point were corrected for defocus, and the change in total RMS was computed and plotted as a function of wavelength as shown in Figures 18 and 19. The behavior of total RMS of both the 193nm lens and the 248nm lenses are a strong function of the strong X-Tilt component. Table 5 shows the peak rates of change for each system.

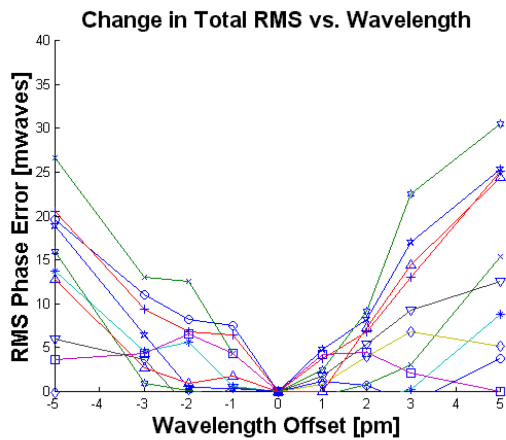

Figure 18. Change in total RMS across wavelength and slit position for 193nm lens.

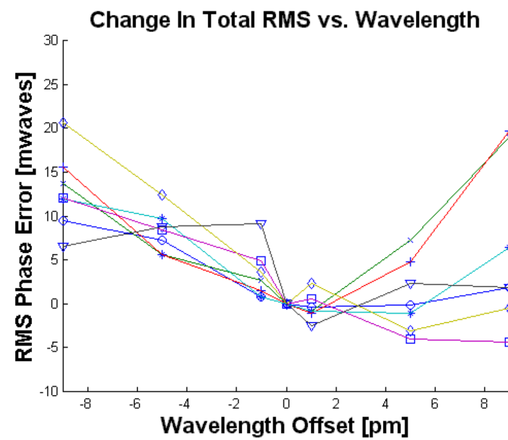

Figure 19. Change in total RMS across wavelength and slit position for 248nm lens.

	Peak Rate of Change In Total RMS [mwaves/pm]
193nm	6.7
248nm	2.2

Table 5. Peak rates of change for total RMS.

4.0 EFFECTS ON IMAGING

4.1 Image Plane

4.1.1 Image Plane Shift

The rate of change of Z4 given in Table 1 can be converted to a rate of change in the image plane (Z position) by

$$\frac{\Delta Z}{\Delta\lambda} = \frac{\Delta Z4}{\Delta\lambda}\frac{\Delta Z}{\Delta Z4}(NA,\lambda) \tag{1}$$

where Z is the position along the optical axis, λ, is the wavelength, Z4 is the Zernike coefficient for defocus and the term $\Delta Z/\Delta Z4(NA,\lambda)$ is a numerical constant dependent upon NA and wavelength[2]. The calculated rates of change for both 193nm and 248nm systems, along with the sensitivity ratio of ArF to KrF is shown in Table 6. The sensitivity ratio is a rough estimate of the laser bandwidth requirement ratio for these particular KrF and ArF systems.

	248nm	193nm
Change in Z position (From Z4)	251.6 nm/pm	291.2 nm/pm
Ratio of ArF to KrF Sensitivity	1.16	

Table 6. Change in Z-position with wavelength for 248nm and 193nm scanner lenses.

4.1.2 Image Plane Deviation

The Z4 terms from the wavelength experiments were converted to z positions in order to estimate the change in across field image plane deviation with wavelength for both the 248nm and 193nm systems. The range of the values of z-positions was determined for each field point, and plotted in Figure 20. The data indicates variation on the order of the wafer flatness spec. No correlation with wavelength was observed.

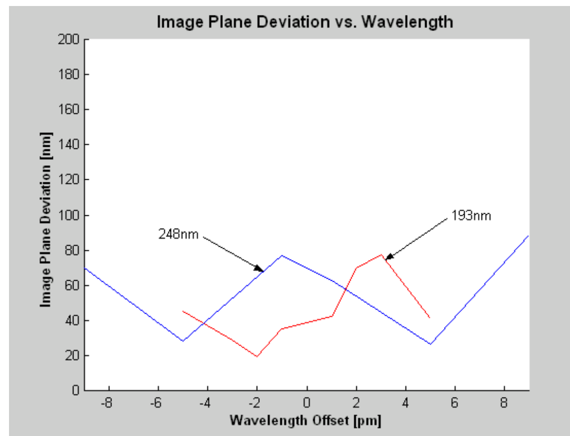

Figure 20. IPD as a function of wavelength for the 193nm and 248nm lenses.

4.2 Image Placement Error

Considering the non-radially symmetric Zernike terms, changing the wavelength produced the most significant change in the tilt terms, Z2 and Z3. The effect of wavefront tilt (Z2, Z3) on feature placement is to create a shift (Δx, Δy) given by

$$(\Delta x, \Delta y) = \lambda o/\pi \ NA \ (Z2, Z3) \quad (2)$$

where λo is the nominal laser wavelength, NA the numerical aperture and (Z2, Z3) the wavefront tilts in radians. The effect of the strong Z2 wavelength dependence shown in Figures 9 and 11 is to create a wavelength dependent distortion component in the x-direction that is a combination of x-scale error and x^3. That is, a wavelength shift will produce a distortion of the form:

$$\delta x(x) = (\lambda\text{-}\lambda o)\ x\ dSx/d\lambda + (\lambda\text{-}\lambda o)\ x^3\ dE/d\lambda \quad (3)$$

where δx(x) = laser wavelength induced (chromatic) distortion in the x-direction as a function of intra-field position x, λ-λo = laser wavelength offset, dSx/dλ is the differential x scale, and dE/dλ are the cubic distortion coefficients.

For the 193 nm case, we have computed the expected x displacement rate of change with wavelength as a function of slit position, and plotted the results in Figure 21. The peak rate of change is ~ 4nm/pm.

Figure 21. IPE rate of change as a function of slit position for the 193nm lens.

In order to take into account the partially coherent imaging effects and the effect of the change in the total wavefront, we input the differential wavefronts from the experiments into a lithographic simulator, and simulated image placement error using the max NA and .75 sigma for both the 248nm and 193nm lenses. Figures 22 and 23 show the results of the simulations. For the 193nm case, the simulated results show an x image placement error of ~ 6nm/pm peak rate of change which differs slightly from the ~ 4nm/pm peak rate calculated considering only tilt.

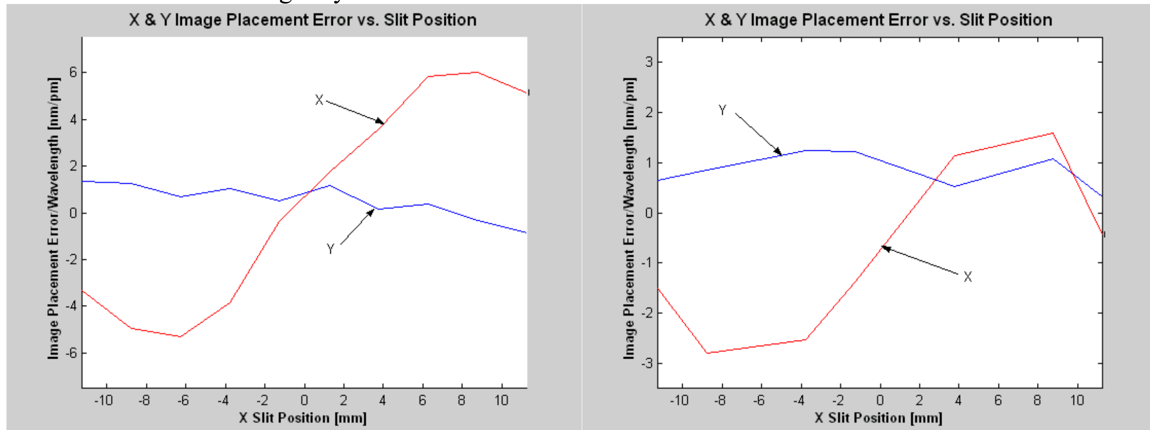

Figure 22. Rate of change in IPE as a function of slit position for the 193nm lens.

Figure 23. Rate of change of IPE as a function of slit position for the 248nm lens.

5.0 CONCLUSION

The effects of varying the wavelength on Zernike polynomials 2-28 as measured by the Litel ISI have been quantified. The largest effects were found to be on the radially symmetric terms Z4, Z11, and Z22. In addition, other effects in the theta dependent terms were also identified and quantified. It was found that the Zernike coefficients for the 193nm system were in general more sensitive to a change in wavelength than the Zernike coefficients for the 248nm system. Across field affects were observed and quantified in Zernike terms Z2 and Z8. Estimates of image placement error were computed by estimating the effect of Z2 only, and also by inputing the total differential wavefronts into a lithographic simulator.

REFERENCES

1. V. N. Mahajan, “Zernike Polynomials and Optical Aberrations of Systems with Circular Pupils,” Engineering Laboratory Notes in Supplement to Applied Optics, December 1994, pp. 8121-8124.
2. A. Suzuki, “Chromatic Aberration,” Canon Sub Micron Focus, Volume 6, Issue 1, pp 5-6, 2001.
3. M. Terry, A. Smith, K. Rebitz, “Gauging the Performance of an In-Situ Interferometer,” Proc. SPIE Volume 4000, Optical Microlithography XIII, pp 1223-1236, 2000.